16 June 1994

PHYSICS LETTERS B

ELSEVIER

Physics Letters B 329 (1994) 399–406

Measurement of the spin-dependent structure function $g_1(x)$ of the proton

Spin Muon Collaboration

D. Adams [s], B. Adeva [u], E. Arik [b], A. Arvidson [x], B. Badelek [x,z], M.K. Ballintijn [p], G. Bardin [t], G. Baum [a], P. Berglund [i], L. Betev [n], I.G. Bird [t,1], R. Birsa [w], P. Björkholm [x], B.E. Bonner [s], N. de Botton [t], F. Bradamante [w], A. Bressan [w], A. Brüll [g,3], S. Bültmann [a], E. Burtin [t], C. Cavata [t], M. Clocchiatti [w], M.D. Corcoran [s], D. Crabb [y], J. Cranshaw [s], M. Crawford [d], T. Çuhadar [b], S. Dalla Torre [w], R. van Dantzig [p], S. Dhawan [aa], C. Dulya [c], A. Dyring [x], S. Eichblatt [s], J.C. Faivre [t], D. Fasching [r], F. Feinstein [t], C. Fernandez [u,j], B. Frois [e,t], J.A. Garzon [u,j], T. Gaussiran [s], M. Giorgi [w], E. von Goeler [q], G. Gracia [u], N. de Groot [p], M. Grosse Perdekamp [c], E. Gülmez [b], D. von Harrach [ℓ], T. Hasegawa [o,5], P. Hautle [f,4], N. Hayashi [o], C.A. Heusch [d], N. Horikawa [o], V.W. Hughes [aa], G. Igo [c], S. Ishimoto [o,6], T. Iwata [o], E.M. Kabuß [ℓ], R. Kaiser [g], A. Karev [k], H.J. Kessler [g], T.J. Ketel [p], A. Kishi [o], Yu. Kisselev [k], L. Klostermann [p], D. Krämer [a], V. Krivokhijine [k], V. Kukhtin [k], J. Kyynäräinen [e,i], M. Lamanna [w], U. Landgraf [g], K. Lau [j], T. Layda [d], J.M. Le Goff [t], F. Lehar [t], A. de Lesquen [t], J. Lichtenstadt [v], T. Lindqvist [x], M. Litmaath [p], S. Lopez-Ponte [u,j], M. Lowe [s], A. Magnon [e,t], G.K. Mallot [ℓ,e], F. Marie [t], A. Martin [w], J. Martino [t], T. Matsuda [o,5], B. Mayes [j], J.S. McCarthy [y], K. Medved [k], G. van Middelkoop [p], D. Miller [r], K. Mori [o], J. Moromisato [q], A. Nagaitsev [k], J. Nassalski [z], L. Naumann [e], T.O. Niinikoski [e], J.E.J. Oberski [p], D.P. Parks [j], A. Penzo [w], C. Perez [u], F. Perrot-Kunne [t], D. Peshekhonov [k], R. Piegaia [e,aa,7], L. Pinsky [j], S. Platchkov [t], M. Plo [u], D. Pose [k], H. Postma [p], J. Pretz [ℓ], T. Pussieux [t], J. Pyrlik [j], I. Reyhancan [b], J.M. Rieubland [e], A. Rijllart [e], J.B. Roberts [s], S. Rock [e,9], M. Rodriguez [u], E. Rondio [z], A. Rosado [n], I. Sabo [v], J. Saborido [u], A. Sandacz [z], I. Savin [k], P. Schiavon [w], K.P. Schüler [aa,8], R. Segel [r], R. Seitz [ℓ], Y. Semertzidis [e], F. Sever [p,10], P. Shanahan [r], N. Shumeiko [19], G. Smirnov [k], A. Staude [n], A. Steinmetz [ℓ], U. Stiegler [e], H. Stuhrmann [h], K.M. Teichert [n], F. Tessarotto [w], M. Velasco [r], J. Vogt [n], R. Voss [e], R. Weinstein [j], C. Whitten [c], R. Windmolders [m], R. Willumeit [h], W. Wislicki [z], A. Witzmann [g], A.M. Zanetti [w], J. Zhao [h]

[a] *University of Bielefeld, Physics Department, 33501 Bielefeld, Germany* [11]

[b] *Bogaziçi University and Çeknece Nuclear Research Center, Istanbul, Turkey*

[c] *University of California, Department of Physics, Los Angeles, 90024 CA, USA* [12]

[d] *University of California, Institute of Particle Physics, Santa Cruz, 95064 CA, USA*

[e] *CERN, 1211 Geneva 23, Switzerland*

[f] *ETH, 8093 Zürich, Switzerland*

Elsevier Science B.V.
SSDI 0370-2693(93)0370-2693(94)00504-Z

[g] University of Freiburg, Physics Department, 79104 Freiburg, Germany[11]
[h] GKSS, 21494 Geesthacht, Germany[11]
[i] Helsinki University of Technology, Low Temperature Laboratory, Otakaari 3A, 02150 Finland
[j] University of Houston, Department of Physics, Houston, 77204-5504 TX, and Institute for Beam Particle Dynamics, Houston, 77204-5506 TX, USA[12,13]
[k] JINR, Laboratory of Super High Energy Physics, Dubna, Russia
[ℓ] University of Mainz, Institute for Nuclear Physics, 55099 Mainz, Germany[11]
[m] University of Mons, Faculty of Science, 7000 Mons, Belgium
[n] University of Munich, Physics Department, 80799 Munich, Germany[11]
[o] Nagoya University, Department of Physics, Furo-Cho, Chikusa-Ku, 464 Nagoya, Japan[14]
[p] NIKHEF, Delft University of Technology, FOM and Free University, 1009 AJ Amsterdam, The Netherlands[15]
[q] Northeastern University, Department of Physics, Boston, 02115 MA, USA[13]
[r] Northwestern University, Department of Physics, Evanston, 60208 IL, USA[12,13]
[s] Rice University, Bonner Laboratory, Houston, 77251-1892 TX, USA[12]
[t] DAPNIA, C.E. Saclay, 91191 Gif-sur-Yvette, France
[u] University of Santiago, Department of Particle Physics, 15706 Santiago de Compostela, Spain[16]
[v] Tel Aviv University, School of Physics, 69978 Tel Aviv, Israel[17]
[w] INFN Trieste and University of Trieste, Department of Physics, 34127 Trieste, Italy
[x] Uppsala University, Department of Radiation Sciences, 75121 Uppsala, Sweden
[y] University of Virginia, Department of Physics, Charlottesville, 22901 VA, USA[13]
[z] Warsaw University and Soltan Institute for Nuclear Studies, 00681 Warsaw, Poland[18]
[aa] Yale University, Department of Physics, New Haven, 06511 CT, USA[12]

Received 9 April 1994
Editor: L. Montanet

Abstract

We have measured the spin-dependent structure function g_1^p of the proton in deep inelastic scattering of polarized muons off polarized protons, in the kinematic range $0.003 < x < 0.7$ and $1\,\mathrm{GeV}^2 < Q^2 < 60\,\mathrm{GeV}^2$. Its first moment, $\int_0^1 g_1^p(x)\,dx$, is found to be 0.136 ± 0.011 (stat.) ± 0.011 (syst.) at $Q^2 = 10\,\mathrm{GeV}^2$. This value is smaller than the prediction of the Ellis–Jaffe sum rule by two standard deviations, and is consistent with previous measurements. A combined analysis of all available proton, deuteron and neutron data confirms the Bjorken sum rule to within 10% of the theoretical value.

The spin dependent structure functions of the nucleon, g_1 and g_2, can be measured in polarized deep inelastic lepton-nucleon scattering [1]. Measurements of g_1 for the proton and the neutron allow us to test a fundamental QCD sum rule, derived by Bjorken [2], and to study the internal spin structure of the nucleon. Ellis and Jaffe [3] have derived sum rules for the pro-

[1] Now at CERN, 1211 Geneva 23, Switzerland
[2] Now at University of Montreal, PQ, H3C 3J7, Montreal, Canada
[3] Now at Max Planck Institute, Heidelberg, Germany
[4] Permanent address: Paul Scherrer Institut, 5232 Villigen, Switzerland
[5] Permanent address: Miyazaki University, 88921 Miyazaki-Shi, Japan
[6] Permanent address: KEK, 305 Ibaraki-Ken, Japan
[7] Permanent address: University of Buenos Aires, Physics Department, 1428 Buenos Aires, Argentina
[8] Now at SSC Laboratory, Dallas, 75237 TX, USA
[9] Permanent address: The American University, Washington D.C. 20016, USA.
[10] Present address: ESFR, F-38043 Grenoble, France.
[11] Supported by Bundesministerium für Forschung und Technologie
[12] Supported by the Department of Energy
[13] Supported by the National Science Foundation
[14] Supported by Ishida Foundation, Mitsubishi Foundation and Monbusho International Science Research Program
[15] Supported by the National Science Foundation (NWO) of the Netherlands
[16] Supported by Comision Interministerial de Ciencia y Tecnologia
[17] Supported by the US-Israel Binational Science Foundation, Jerusalem, Israel and The Israeli Academy of Sciences
[18] Supported by KBN grant nr. 20958-9101
[19] Permanent address: Belarussian State University, Minsk, Belarus.

ton and for the neutron, under the assumptions that the strange sea is unpolarized and that SU(3) symmetry is valid for the baryon octet decays.

First measurements of g_1^p were performed by experiments at SLAC (E80 and E130 [4]) and at CERN (EMC [5]). The analysis of these data [6,5] showed a deviation from the Ellis–Jaffe prediction, with the implications that the total contribution of quark spins to the nucleon spin is small and that the strange sea is negatively polarized. Recently, two experiments have measured g_1^d from polarized muon-deuteron (SMC [7] at CERN) and g_1^n from polarized electron-^{3}He scattering (E142 [8] at SLAC). The conclusions from these two experiments appeared to be at variance. However, combined analyses [9–12] showed that the experimental data agree in the kinematic region of overlap, and emphasized that the conclusions are very sensitive to the small-x extrapolation of $g_1(x)$ and to higher order and higher twist QCD corrections. Additional data are required to provide a more stringent test of the sum rules and to clarify the contribution of the quark spins to the nucleon spin.

In this paper, we report the results of a new measurement of g_1^p at CERN, where longitudinally polarized muons were scattered from longitudinally polarized protons in the kinematic range $1\,\mathrm{GeV}^2 < Q^2 < 60\,\mathrm{GeV}^2$ and $0.003 < x < 0.7$. The experiment is similar to the previous SMC experiment with a deuteron target [7].

The positive muon beam had an intensity of 4×10^7 muons/spill with a spill time of 2.4 s, a period of 14.4 s, and an average muon energy of 190 GeV. The beam polarization was determined from the the shape of the energy spectrum of positrons from the decay $\mu^+ \rightarrow e^+\nu_e\bar{\nu}_\mu$. The polarimeter is described in Ref. [13]. The polarization was measured to be $P_\mu = -0.803 \pm 0.029\,(\mathrm{stat.}) \pm 0.020\,(\mathrm{syst.})$, in good agreement with Monte Carlo simulations of the beam transport [14].

A new polarized target was built for this experiment. Its design is similar to that used in the earlier EMC proton [5] and SMC deuteron [7] experiments. The target consists of an upstream and a downstream cell, each 60 cm long and 5 cm in diameter, separated by 30 cm, and with opposite longitudinal polarizations. The target material was butanol with about 5% of water, in which paramagnetic complexes [15] were dissolved, resulting in a concentration of 7.2×10^{19} unpaired electrons per cm^3. The material was frozen into beads of about 1.5 mm diameter.

A new superconducting magnet system [16] and a new ^{3}He/^{4}He dilution refrigerator were constructed. The magnet system consists of a solenoid, 16 correction coils, and a dipole. The solenoid provides a magnetic field of 2.5 T with its axis aligned along the beam direction and with an homogeneity of 2×10^{-5} throughout the target volume. The dipole magnet provides a magnetic field of up to 0.5 T in the vertical direction. The dilution refrigerator achieved a temperature of about 0.3 K with a cooling power of 0.3 W when polarizing. The typical temperature in frozen spin operation was below 60 mK.

Protons were polarized by dynamic nuclear polarization (DNP). This was obtained by applying microwave power near the resonance frequency of the paramagnetic molecules. To achieve opposite proton polarizations in the two target cells simultaneously, we used slightly different microwave frequencies. In addition, frequency modulation of the microwaves reduced the polarization buildup time by about 20% and increased the maximum polarization by 6%. The mean polarization throughout the data-taking was 0.86, with a maximum value of 0.94.

The measurement of the proton polarization, P_T, was performed with 10 coils along the target using continuous-wave NMR with series Q-meter circuits [17,18]. The NMR signals were calibrated by measuring the thermal equilibrium signals at different temperatures around 1 K, where the natural polarization ($\simeq 0.25\%$) is known from the Curie law. The thermal equilibrium signals were corrected for systematic effects including a small change in size with the field polarity and the contamination with background signals. The signals were also corrected for Q-meter nonlinearity effects present at large polarizations. The relative accuracy of the polarization measurement was 3%.

The spin directions were reversed every 5 hours with only small losses of polarization and running time, by rotating the magnetic field direction using a superposition of the solenoid and the dipole fields. In addition, the spin polarization in each target cell was reversed via DNP once a week. During spin reversals by field rotation, the field was made slightly inhomogeneous to avoid depolarization due to superradiance [19].

The momentum of the incident muon was measured

using a bending magnet upstream of the target. Its track was reconstructed from hits in scintillator hodoscopes and proportional chambers. The trajectory and the momentum of the scattered muon were determined from hits in a total of 150 planes of proportional chambers, drift chambers and streamer tubes located upstream and downstream of the forward spectrometer magnet (FSM). The large number of planes minimized the effect of individual plane inefficiencies on the overall track reconstruction efficiency. The scattered muon was identified by having traversed a 2 m thick hadron absorber made of iron. Incident and scattered muon tracks determined the interaction vertex with an average resolution of 30 mm (0.3 mm) in the direction parallel (perpendicular) to the beam direction.

The readout of the apparatus was triggered by coincident hits in three large scintillator hodoscopes, one located just downstream of the FSM and two located downstream of the hadron absorber. A dedicated trigger for events with small scattering angles used hodoscopes with finer segmentation close to the beam and covered mainly the small x range.

Cuts were applied to minimize smearing effects, to limit the size of radiative corrections, to reject muons originating from the decay of pions produced in the target, to ensure that the beam flux was the same for both target cells and to ensure proper separation of events originating from the upstream and downstream target cells. After cuts, the data sample amounted to 3.1×10^6 events and 1.3×10^6 events for the large and small angle triggers, respectively.

The virtual-photon proton asymmetry A_1^p is related to the measured muon-proton asymmetry $A^p = (\sigma^{\uparrow\downarrow} - \sigma^{\uparrow\uparrow})/(\sigma^{\uparrow\downarrow} + \sigma^{\uparrow\uparrow})$ by [1]

$$A_1^p = \frac{\sigma_{1/2} - \sigma_{3/2}}{\sigma_{1/2} + \sigma_{3/2}} = \frac{A^p}{D} - \eta A_2^p, \tag{1}$$

where $1/2$ and $3/2$ are the total spin projections in the direction of the virtual photon. The depolarization factor D and the coefficient η depend on the event kinematics. In addition, D depends on the unpolarized structure function $R(x, Q^2)$, which was taken from a global fit of the SLAC data [20]. The asymmetry A_2^p arises from the interference between transverse and longitudinal virtual photon polarizations and is constrained by the positivity limit $|A_2^p| \leq \sqrt{R}$. We have measured A_2^p in a dedicated experiment, where the dipole field was used to hold the proton polarization in a direction perpendicular to the beam. We found A_2^p to be compatible with zero within a statistical uncertainty of 0.20, which is a stronger constraint than the one imposed by the positivity limit. In addition, since the coefficient η is small in the kinematic range covered by our experiment, we neglected the term ηA_2^p and included its possible effect in the systematic error.

The asymmetry A_1^p is extracted from combinations of data sets taken before and after a polarization reversal. Each event is weighted with the corresponding values of D and the dilution factor f, the fraction of the event yield from protons of hydrogen in the target ($f \simeq 0.12$). Since we take data simultaneously with oppositely polarized cells, the incident muon flux, the amount of material in the target cells and the absolute value of the spectrometer acceptances, a_u and a_d, cancel in the determination of A_1^p. The subscripts u and d refer to the upstream and downstream target cells, respectively. The only assumption in deriving A_1^p is that the ratio $r = a_u/a_d$ remains constant within the typical period of time between two polarization reversals ($\Delta t \simeq 5$ hours). A time dependence of r leads to a false asymmetry of

$$\Delta A_1^p = \frac{1}{4 f P_\mu P_T D} \frac{\Delta r}{r}, \tag{2}$$

In order to estimate the uncertainty due to this effect, we have studied the time dependences of all detector efficiencies; we then reprocessed the data after artificially imposing on the whole sample the largest of the variations observed within two polarization reversals. We also reanalyzed the data ignoring the information from a fraction of the planes in our chambers. In this way, we artificially reduced the redundancy of the spectrometer and became more sensitive to time dependences. Finally, we divided the data into different subsets according to a variety of criteria (e.g. data-taking periods, radial vertex position, events reconstructed in different parts of the spectrometer) and looked for disagreements between the different samples. From these studies we concluded that $\Delta r/r < 7 \times 10^{-4}$, corresponding to a false asymmetry $\Delta A_1^p < 7 \times 10^{-3}$.

Spin-dependent radiative corrections to A_1^p were calculated using the approach of Ref. [21]. They were found to be small over the whole kinematic range. The

Table 1
Results on the virtual photon proton asymmetry A_1^p and the spin structure function g_1^p of the proton

x-range	$\langle x \rangle$	$\langle Q^2 \rangle$ (GeV^2)	A_1^p	g_1^p	g_1^p (Q^2=10GeV^2)
0.003–0.006	0.005	1.3	0.053±0.025±0.007	1.34±0.62±0.27	2.48±1.15±0.49
0.006–0.010	0.008	2.1	0.042±0.024±0.005	0.73±0.42±0.11	1.13±0.65±0.17
0.010–0.020	0.014	3.7	0.048±0.022±0.005	0.52±0.24±0.06	0.67±0.31±0.08
0.020–0.030	0.025	6.0	0.050±0.031±0.005	0.34±0.21±0.03	0.38±0.24±0.04
0.030–0.040	0.035	8.1	0.069±0.039±0.006	0.35±0.20±0.03	0.37±0.20±0.03
0.040–0.060	0.049	10.8	0.124±0.034±0.009	0.46±0.13±0.03	0.45±0.13±0.03
0.060–0.100	0.077	15.5	0.161±0.035±0.012	0.38±0.08±0.03	0.36±0.08±0.03
0.100–0.150	0.122	22.1	0.275±0.047±0.019	0.40±0.07±0.03	0.38±0.06±0.03
0.150–0.200	0.172	28.5	0.273±0.067±0.020	0.26±0.06±0.02	0.25±0.06±0.02
0.200–0.300	0.241	36.3	0.267±0.070±0.022	0.16±0.04±0.01	0.16±0.04±0.01
0.300–0.400	0.342	46.4	0.529±0.115±0.043	0.17±0.04±0.01	0.18±0.04±0.01
0.400–0.700	0.481	58.0	0.520±0.156±0.049	0.06±0.02±0.01	0.08±0.02±0.01

The first error is statistical, the second one is systematic. For the evaluation of $g_1^p(Q^2 = 10\,\mathrm{GeV}^2)$, it has been assumed that A_1^p does not depend on Q^2.

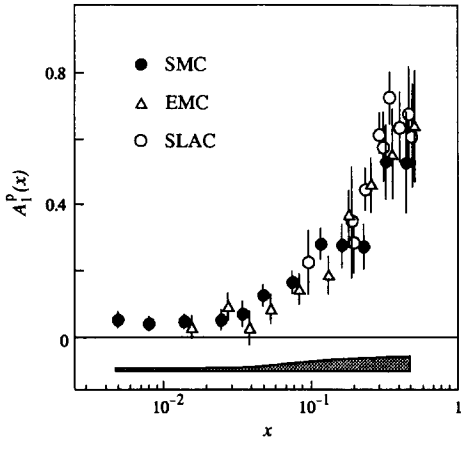

Fig. 1. The virtual-photon proton cross section asymmetry A_1^p as a function of the Bjorken scaling variable x. Only statistical errors are shown with the data points. The size of the systematic errors for the SMC points is indicated by the shaded area.

uncertainty in the radiative corrections arises predominantly from uncertainties in the structure functions used as input. Asymmetries arising from electroweak interference are negligible in the Q^2 range of this experiment.

The results for A_1^p for each x bin at the respective mean Q^2 are given in Table 1, and are shown in Fig. 1. Sources of systematic errors include the uncertainties in the beam and target polarizations, the structure function R, the dilution factor f, the radiative corrections, the momentum measurement, the kinematic smearing corrections, the stability in time of the acceptance ratio, and the neglect of A_2. The different systematic errors were combined in quadrature.

The spin structure function g_1^p was evaluated from the average asymmetry A_1^p in each x bin using the relation

$$g_1^p(x,Q^2) = \frac{A_1^p(x,Q^2)F_2^p(x,Q^2)}{2x[1+R(x,Q^2)]}. \qquad (3)$$

The unpolarized structure function, $F_2^p(x,Q^2)$, was taken from the NMC parametrization [22]. The uncertainty is typically 3% to 5%. The lowest x bin is outside the kinematic region covered by the NMC data, but we have verified that their parametrization extrapolates smoothly to the HERA data [23], and estimated the corresponding uncertainty to be 15%. The structure function g_1^p is practically independent of R due to cancellations between the implicit R dependences in D and F_2 and the explicit one in Eq. (3). Results for g_1^p are given in Table 1 and Fig. 2.

To evaluate the integral $\int g_1^p(x,Q_0^2)dx$ at a fixed Q^2, we recalculated g_1^p at $Q_0^2 = 10\,\mathrm{GeV}^2$, which represents an average value for our data. Using Eq. 3, we obtained $g_1^p(x,Q_0^2)$ in each bin assuming $A_1(x,Q^2)$ to be independent of Q^2. This assumption is consistent with our data, with previous experimental results for both the proton [5] and deuteron [7], and with recent theoretical calculations [11]. The values of $g_1^p(x,Q_0^2)$

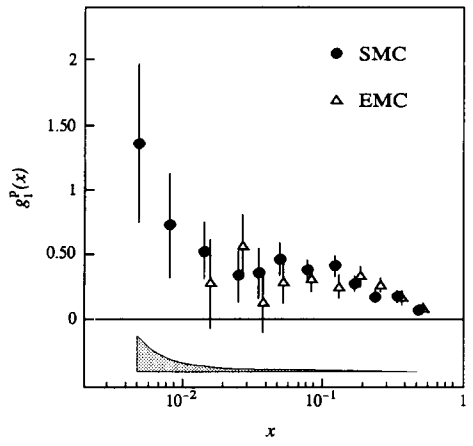

Fig. 2. The solid circles (right-hand axis) show the structure function xg_1^p as a function of the Bjorken scaling variable x, at $Q_0^2 = 10\,\mathrm{GeV}^2$. The open boxes (left-hand axis) show $\int_{x_m}^1 g_1^p(x)dx$, where x_m is the value of x at the lower edge of each bin. Only statistical errors are shown. The solid square shows our result $\int_0^1 g_1^p(x)dx$, with statistical and systematic errors combined in quadrature. Also shown is the theoretical prediction by Ellis and Jaffe [3].

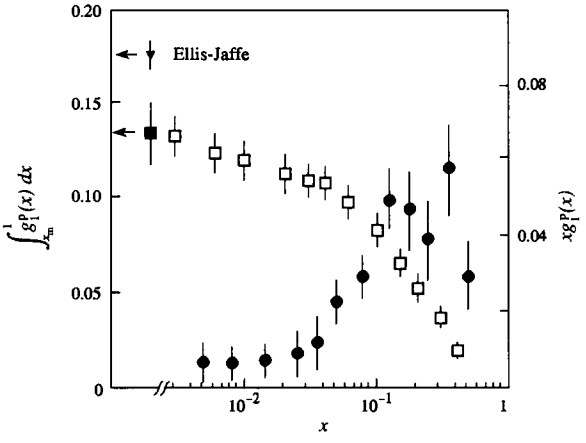

Fig. 3. The spin dependent structure function $g_1^p(x)$ at the average Q^2 of each x bin (Table 1). Only statistical errors are shown with the data points. The size of the systematic errors for the SMC data is indicated by the shaded area. The EMC points are reevaluated using the NMC F_2 parametrization [22].

are shown in Table 1.

The integral over the measured x range is

$$\int_{0.003}^{0.7} g_1^p(x, Q_0^2)dx = 0.131 \pm 0.011 \pm 0.011. \qquad (4)$$

Here, and in the following, the first error is statistical and the second is systematic. The contributions to the systematic error are detailed in Table 2.

To estimate the integral for $x > 0.7$, we take $A_1^p = 0.7 \pm 0.3$ for $0.7 < x < 1.0$, which is consistent with the bound $A_1 < 1$, and also with the result from perturbative QCD [24] that $A_1 \to 1$ as $x \to 1$. This contribution amounts to 0.0015 ± 0.0007. The integral $\int_{x_m}^1 g_1^p(x)dx$ as a function of the lower integration limit, x_m, is shown in Fig. 3. The contribution to the integral from the unmeasured region $x < 0.003$ was evaluated assuming a Regge-type dependence $g_1^p(x) = constant$ [25], that we fit to our two lowest x data points. We obtain $\int_0^{0.003} g_1^p(x)dx = 0.004 \pm 0.002(\mathrm{stat.})$. We increase this error to 0.004 so that it covers the results obtained when either the lowest x point or the three lowest x points are used to determine the extrapolation. This range also covers the results obtained using the general form of Regge dependence $g_1^p(x) \propto x^\alpha$, with $0 < \alpha < 0.5$ [25]. Although g_1 shows a tendency to increase at low x, Table 1, we do not consider the trend significant enough to call into question the validity of Regge behavior.

The result for the first moment of $g_1^p(x)$ at $Q_0^2 = 10\,\mathrm{GeV}^2$ is

Table 2
Contributions to the error on Γ_1^p

Source of the error	$\Delta\Gamma_1^p$
Beam polarization	0.0057
Uncertainty on F_2	0.0052
Extrapolation at low x	0.0040
Target polarization	0.0039
Dilution factor	0.0034
Acceptance variation Δr	0.0030
Radiative corrections	0.0023
Neglect of A_2	0.0017
Momentum measurement	0.0020
Uncertainty on R	0.0018
Kinematic resolution	0.0010
Extrapolation at high x	0.0007
Total systematic error	0.0113
Statistics	0.0114

$$\Gamma_1^p(Q_0^2) = \int_0^1 g_1^p(x, Q_0^2)\,dx = 0.136 \pm 0.011 \pm 0.011. \quad (5)$$

The Ellis–Jaffe sum rule, including first order QCD corrections [26], predicts $\Gamma_1^p = 0.176 \pm 0.006$ for $\alpha_s(10\,\mathrm{GeV}^2) = 0.23 \pm 0.02$, corresponding to $\alpha_s(M_Z^2) = 0.113 \pm 0.004$ [27] and four quark flavors. Our measurement is two standard deviations below this value.

The first moment Γ_1^p can be expressed in terms of the proton matrix element of the flavor singlet axial vector current a_0 [5] and the SU(3) coupling constants F and D [28]. We obtain $a_0 = 0.18 \pm 0.08 \pm 0.08$. In the quark-parton model, a_0 is proportional to $\Delta\Sigma = \Delta u + \Delta d + \Delta s$, the sum of the quark spin contributions to the nucleon spin. Our result corresponds to

$$\Delta\Sigma = 0.22 \pm 0.10 \pm 0.10 \quad (6)$$

and

$$\Delta s = -0.12 \pm 0.04 \pm 0.04. \quad (7)$$

We thus find that only a small fraction of the nucleon spin is due to the helicity of the quarks, and that the strange sea is negatively polarized.

Our results are in good agreement with the previous measurements of E80/E130 and the EMC. A test of consistency of the experimental asymmetries $A_1^p(x)$ from all experiments yields $\chi^2 = 14.6$ for 15 degrees of freedom. To compare g_1^p, values we apply to the EMC asymmetries the same F_2^p parametrization that we use in the present work. An evaluation of the integral over the x range common to both experiments, at $Q_0^2 = 10\,\mathrm{GeV}^2$, yields $\int_{0.01}^{0.7} g_1^p(x)\,dx = 0.124 \pm 0.013 \pm 0.019$ for the EMC and $\int_{0.01}^{0.7} g_1^p(x)\,dx = 0.118 \pm 0.010 \pm 0.009$ for our data. In the range $0 < x < 0.01$, the extrapolation of the EMC data gives 0.003 ± 0.003, while our two lowest x points and our extrapolation give $\int_0^{0.01} g_1^p(x)\,dx = 0.017 \pm 0.006$.

For a common evaluation of Γ_1^p from all existing data, we combine our results on $A_1^p(x)$ with those of E80/E130 and EMC. The extrapolations are recalculated from the combined asymmetries following the methods described above. The treatment of the systematic errors takes into account that some of them are correlated between the different experiments. This yields

$$\Gamma_1^p(10\,\mathrm{GeV}^2) = 0.142 \pm 0.008 \pm 0.011 \quad \textit{(All proton data)}, \quad (8)$$

which is two standard deviations below the Ellis–Jaffe prediction. From this result, we obtain $\Delta\Sigma = 0.27 \pm 0.08 \pm 0.10$ and $\Delta s = -0.10 \pm 0.03 \pm 0.04$.

We now turn to a test of the Bjorken sum rule [2], using all available proton, neutron and deuteron data. We do this test at $Q^2 = 5\,\mathrm{GeV}^2$ in order to avoid a large Q^2 evolution of the SLAC-E142 neutron data, which have an average $Q^2 = 2\,\mathrm{GeV}^2$. A fit to Γ_1^p (Eq. 8), Γ_1^n [8] and Γ_1^d [7], reevaluated at $5\,\mathrm{GeV}^2$ under the assumption that the asymmetries A_1 are independent of Q^2, yields

$$\Gamma_1^p - \Gamma_1^n = 0.163 \pm 0.017 \qquad (Q^2 = 5\,\mathrm{GeV}^2), \quad (9)$$

where statistical and systematic errors are combined in quadrature. When one uses the available deuteron and proton data to replace the extrapolation on the neutron data, as discussed in Ref. [12], one obtains $\Gamma_1^n = -0.069 \pm 0.025$ and

$$\Gamma_1^p - \Gamma_1^n = 0.204 \pm 0.029 \qquad (Q^2 = 5\,\mathrm{GeV}^2), \quad (10)$$

with a larger error due to the limited statistics in the deuteron experiment. The theoretical prediction, including perturbative QCD corrections up to third order in α_s [29], gives

$$\Gamma_1^p - \Gamma_1^n = 0.185 \pm 0.004 \qquad \textit{(Theory)} \quad (Q^2 = 5\,\mathrm{GeV}^2), \quad (11)$$

which is in agreement with the above experimental results. Higher-twist effects are expected to contribute especially at low Q^2 [30,31], and have been estimated [11,31] to change $\Gamma_1^p - \Gamma_1^n$ by about 2%, but the calculations are model dependent. We have therefore not taken these contributions into account.

In summary, we have presented a new measurement of the proton spin dependent structure function g_1^p. The measured asymmetries are in agreement with those of the earlier E80/E130 and EMC experiments, but systematic errors have been significantly reduced and the kinematic region has been extended down to $x = 0.003$.

The first moment of the spin dependent structure function g_1^p, evaluated from our own data, is two standard deviations below the prediction of the Ellis–Jaffe sum rule. In the quark parton model, this result implies that the contribution of the quark spins to the proton spin is 0.22 ± 0.14. The Bjorken sum rule is now confirmed, at the one standard deviation level, to within 10% of its theoretical value.

References

[1] V.W. Hughes and J. Kuti, Ann. Rev. Nucl. Part. Sci. 33 (1983) 611.
[2] J.D. Bjorken, Phys. Rev. 148 (1966) 1467; Phys. Rev. D1 (1970) 1376.
[3] J. Ellis and R.L. Jaffe, Phys. Rev. D9 (1974) 1444; D10 (1974) 1669.
[4] SLAC E-80, M.J. Alguard et al., Phys. Rev. Lett. 37 (1976) 1261; ibid. 41 (1978) 70;
SLAC E-130 G. Baum et al., Phys. Rev. Lett. 51 (1983) 1135.
[5] EMC, J. Ashman et al., Phys. Lett. B206 (1988) 364; Nucl. Phys. B328 (1989) 1.
[6] V.W. Hughes et al., Phys. Lett. B212 (1988) 511.
[7] SMC, B. Adeva et al., Phys. Lett. B302 (1993) 533.
[8] SLAC E142, D.L. Anthony et al., Phys. Rev. Lett. 71 (1993) 959.
[9] J. Ellis and M. Karliner, Phys. Lett. B313 (1993) 131.
[10] F.E. Close and R.G. Roberts, Phys. Lett. B316 (1993) 165.
[11] G. Altarelli, P. Nason and G. Ridolfi, Phys. Lett. B320 (1994) 152.
[12] SMC, B. Adeva et al., Phys. Lett. B320 (1994) 400
[13] SMC, B. Adeva et al., Nucl. Instrum. Methods A343 (1994) 363.
[14] N. Doble et al., Nucl. Instrum. Methods A343 (1994), to be published.
[15] M. Krumpolc and J. Rocek, J. Am. Chem. Soc. 101 (1979) 3206
[16] A. Dael et al., Proceedings of the 12^{th} Magnet Technology Conference, Cryomag 91-05 (1991).
[17] G.R. Court et al., Nucl. Instrum. Methods. A324 (1993) 433.
[18] SMC, B. Adeva et al., CERN-PPE/94-54, Nucl. Instrum. Methods A (1994), to be published.
[19] R.H. Dicke, Phys. Rev. 93 (1954) 99;
Y.F. Kisselev et al., Zh. Eksp. Teor. Fiz. 94 (2) (1988) 344, Sov. Phys. JETP 67 (1988) 413
[20] L.W. Whitlow et al., Phys. Lett. B250 (1990) 193.
[21] T.V. Kukhto and N.M. Shumeiko. Nucl. Phys. B219 (1983)412;
I.V. Akushevich and N.M. Shumeiko. J. Phys. G: Nucl. Phys. 20 (1994) number 4 (to be published).
[22] NMC, P. Amaudruz et al., Phys. Lett. B295 (1992) 159 and preprint CERN-PPE/92-124 (July 1992); Errata Oct. 26 (1992) and Apr. 19 (1993).
[23] M. Derrick et al., Phys. Lett. B316 (1993) 412;
I. Abt et al., Phys. Lett. B321 (1994) 161; Nucl. Phys. B407 (1993) 515.
[24] S.J. Brodsky, M. Burkardt, and I. Schmidt, SLAC PUB 6087 (1994)
[25] R.L. Heimann, Nucl. Phys. B64 (1973) 429;
J. Ellis and M. Karliner, Phys. Lett. B213 (1988) 73.
[26] J. Kodaira et al., Phys. Rev. D20 (1979) 627;
J. Kodaira et al., Nucl. Phys. B159 (1979) 99;
J. Kodaira, Nucl. Phys. B165 (1980) 129.
[27] Particle Data Group, Phys. Rev. D45 (1992) 2.
[28] Z. Dziembowski and J. Franklin, Nucl. Part. Phys. 17 (1991) 213
[29] S.A. Larin and J.A.M. Vermaseren, Phys. Lett. B259 (1991) 345.
[30] I.I. Balitsky, V.M. Braun and A.V. Kolesnichenko, Phys. Lett. B242 (1990) 245 and Erratum, Phys. Lett. B318 (1993) 648.
[31] X. Ji and P. Unrau, MIT-CTP-2232 (1993).